Topological Requirements for CI-M6PR-Mediated Cell Uptake

Lamiaa M A Ali Ab, Matthieu Simon, Khaled El Cheikh, Julie Aguesseau-Kondrotas, Anastasia Godefroy, Christophe Nguyen, Marcel Garcia, Alain Morère, Magali Gary-Bobo, Ludovic Maillard

Supporting Information

Topological Requirements for CI-M6PR-Mediated Cell Uptake

Lamiaa M. A. Ali[ab],‡ Matthieu Simon[a],‡ Khaled El Cheikh[c], Julie Aguesseau-Kondrotas [a], Anastasia Godefroy[ac], Christophe Nguyen[a], Marcel Garcia[c], Alain Morère[a], Magali Gary-Bobo[a], and Ludovic Maillard[a]*

[a] Institut des Biomolécules Max Mousseron, UMR CNRS-UM-ENSCM 5247, UFR des Sciences Pharmaceutiques et Biologiques, 15 Avenue Charles Flahault, 34093 Montpellier Cedex 5, France.

[b] Biochemistry Department, Medical Research Institute, Alexandria University, 21561 Alexandria, Egypt.

[c] NanoMedSyn, Avenue Charles Flahault, 34093 Montpellier cedex 05, France.

N-Fmoc-ATC-OH monomer units and oligomers **4-6** have been synthesized as previously reported.[1, 2]

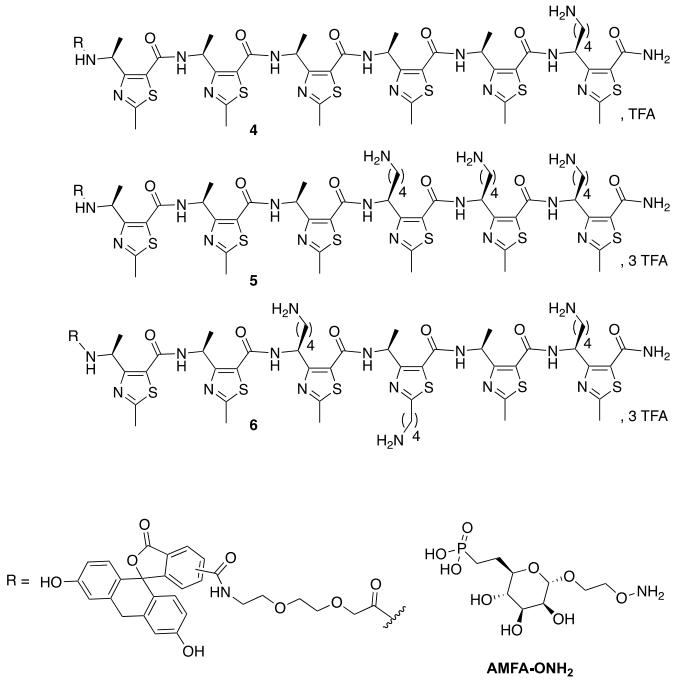

Chart S1. Sequences of the fluorescently labeled ATC oligomers **4**, **5** and **6** and structure of the alcoxyamine analogue of M6P functionalized on aglycon (AMFA-ONH_2).

I. Synthesis of 1-6

Steps a, b, c, d as defined Figure 1A

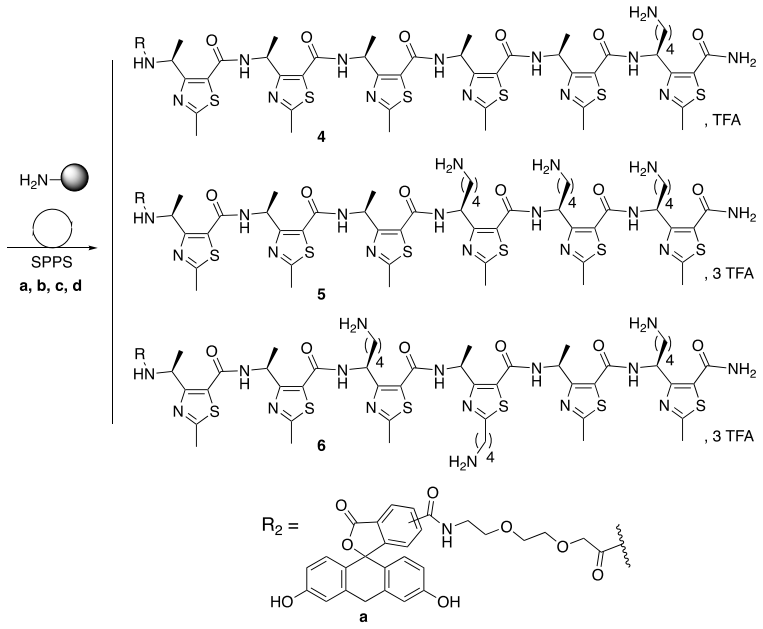

Solid-phase synthesis was performed on a ChemMatrix® Rink Amide resin loaded at 0.49 mmol/g using Fmoc/t-Bu chemistry. Resin was soaked in N-methylpyrrolidone (NMP) for 5-10 min and filtered. Fmoc-ATC-OH (2.0 equiv.), DIC (2.0 equiv.), Oxyma Pure (2.0 equiv.) and NMP were added in this order for each peptide coupling (overnight at r.t.). Resin was washed using the following procedure: 3 × DMF, 3 × DCM, 1 × DMF, 1 × DCM. Each coupling was followed by a capping step with Ac_2O/DCM 1/1 vv solution (1 × 5 min at r.t.) and washed. Deprotection at the N-terminus was performed using a 20% piperidine/DMF solution (3 × 10 min at r.t.) and the resin was then washed before the next coupling. Deprotection and coupling steps were monitored by Kaiser test. N-terminus labeling was done using 8-(Fmoc-amino)-3,6-dioxaoctanoic acid (3.0 equiv.), DIC (3.0 equiv.), Oxyma Pure (3.0 equiv.) in NMP. After Fmoc removal with 20% piperidine/DMF solution (3 × 10 min at r.t.), 5,6-carboxyfluorescein (2.6 equiv.) was coupled to the N-terminus extremity using HBTU (2.6 equiv.) and DIEA (5.0 equiv.) in NMP. The γ-peptide was then cleaved from the resin with a TFA/TIS/H_2O 95/2.5/2.5 vvv solution (2 × 90 min at r.t.). The resin was washed (1 × DCM and 1 × cleavage cocktail) and filtered. The filtrate was evaporated under reduced pressure. ATC oligomer **4-6** as a TFA salt was lyophilized then purified by preparative RP-HPLC on a Waters system controller equipped with a C18 Waters Delta-Pack column (100 × 40 mm, 100 Å) flow 50 mL/min; UV detection at 214 nm using a Waters 486 Tunable

Absorbance Detector and a linear gradient of A = H_2O (0.1 % TFA) and B = CH_3CN (0.1 % TFA).

Steps e, f, g as defined Figure 1A

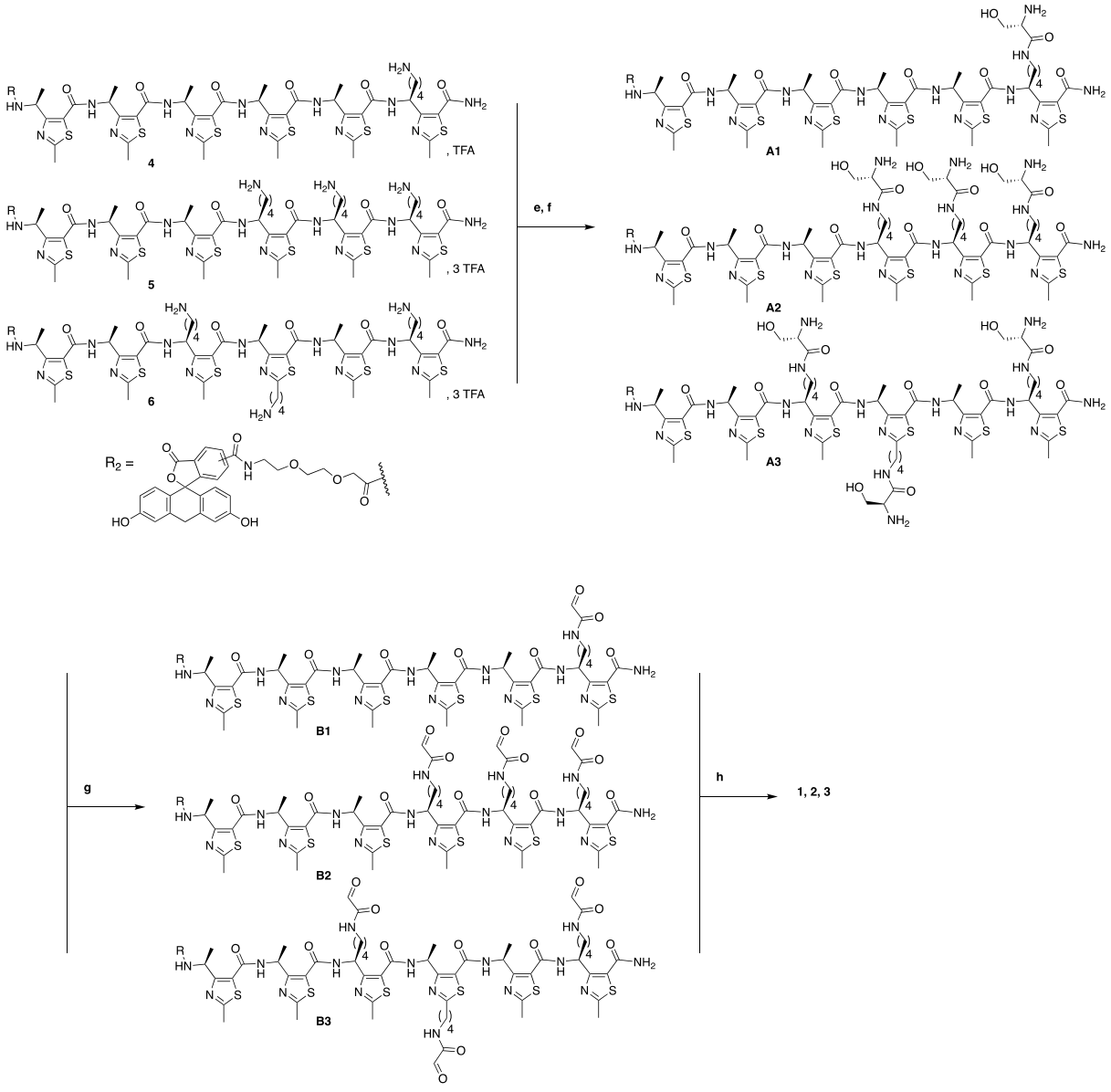

e) Boc-Ser(tBu)-OH, HATU, NMM, DMF/DCM; f) TFA; g) $NaIO_4$, sodium phosphate buffer 50 mM, pH 7.4; h) AMFA-ONH_2,THF/PBS 50mM, pH 5.2

e/ Fmoc-Ser(tBu)-OH (1.2 equiv. relative to the aminoalkyl lateral chains on **4**-**6**) was activated with NMM (5 equiv. relative to the aminoalkyl lateral chains on **4**-**6**) and HATU (1.2 equiv. relative to the aminoalkyl lateral chains on 4-6) for 10 min at rt in DCM/DMF (8:2 vv) (2.5 ml per 0.25 mmol ATC oligomer). Then the mixture was added to a solution of **4**-**6** in DCM (1 mL per 0.25 mmol ATC oligomer). After reaction completion (HPLC monitoring),

the solvent was removed under vaccuo then the reaction mixture was treated with 2 mL aqueous ammonia 32%. After 10 min stirring the solution was lyophilized. The resulting compound was used in the next step without further purification. **f/** Removal of the acido-labile protecting groups was done by mixing the crude product obtained at the previous step with 2 mL TFA for 1 h. Afterward TFA was evaporated under a flow of nitrogen then **A1-3** was solubilized in water/ACN (1:1 vv) and purified by RP-chromatography on a Waters system controller equipped with a C18 Waters Delta-Pack column (100 × 40 mm, 100 Å) flow 50 mL/min; UV detection at 214 nm using a Waters 486 Tunable Absorbance Detector and a linear gradient of A = H_2O (0.1 % TFA) and B = CH_3CN (0.1 % TFA) and then lyophilized (Average isolated yield 20%). **g/ A1-3** was solubilized in 50 mM phosphate buffer pH 7.4 (4 mL) then $NaIO_4$ (1 equiv. relative to lateral chain) was added. After 10 min stirring the reaction was quenched by adding serine (20 equiv.) then **B1-3** was purified by RP-chromatography as described previously and lyophilized (Average isolated yield 30%). **h/** 10 mg of **B1-3** was solubilized in 500 µL of THF/PBS 50mM, pH 5.2, (1:1 vv) then AMFA (3 equiv. relative to aldehyde groups on **B1-3**) solubilized in 100 µL of PBS, 50 mM, pH 5.2 was added to the peptide solution. Reaction was stirred at 37°C during 1-3 days, completion was carefully monitored by LC-MS. Then compounds **1-3** were purified by RP-chromatography as described previously and lyophilized (Average isolated yield 60%).

II. NMR studies

NMR and Molecular modeling studies:

NMR experiments. The NMR samples contained 2 mM of **2** and **3** dissolved in PBS/D2O (95/5), pH 6.8. All spectra were recorded on a Bruker Avance 600 AVANCE III spectrometer equipped with a 5 mm triple-resonance cryoprobe (^{1}H, ^{13}C, ^{15}N). Homonuclear 2-D spectra DQF-COSY, TOCSY (DIPSI2) and ROESY were typically recorded in the phase-sensitive mode using the States-TPPI method as data matrices of 300 real (t_1) × 2048 (t_2) complex data points; 8-32 scans per t_1 increment with 1.2 s recovery delay and spectral width of 7211 Hz in both dimensions were used. The mixing times were 80 ms for TOCSY and 350 ms for the ROESY experiments. In addition, 2D heteronuclear spectra, ^{13}C-HSQC and ^{13}C-HMBC were acquired to fully assign the oligomers (24-32 scans, 256 real (t_1) × 2048-4096 (t_2) complex data points). Spectra were processed with Topspin (Bruker Biospin) and visualized with Topspin or NMRview on a Linux station. The matrices were zero-filled to 1024 (t_1) x 2048 (t_2) points after apodization by shifted sine-square multiplication and linear prediction in the F1 domain. Chemical shifts were referenced to the TMS.

Force field libraries for ATC fragments were generated using the restrained electrostatic potential (RESP) method. Atom charges were derived from the electrostatic potential obtained by DFT calculations with Gaussian 09[3] at the M062X/6-31+G(d) level of theory in vacuum. The computed electrostatic potential (ESP) was fit using RESP charge fitting in antechamber.

^{1}H chemical shifts were assigned according to classical procedures. NOE cross-peaks were integrated and assigned within the NMRView software.[4] The volume of a ROE between methylene pair protons or ortho phenyl protons was used as a reference of 1.8 Å or 2.48 Å respectively. The lower bound for all restraints was fixed at 1.8 Å and upper bounds at 2.7, 3.3 and 5.0 Å, for strong, medium and weak correlations, respectively. Pseudo-atoms corrections of the upper bounds were applied for unresolved aromatic, methylene and methyl protons signals as described previously.[5] Structure calculations were performed with AMBER 16[6] in three stages: cooking, simulated annealing in vacuum and refinement in a solvent box. The cooking stage was performed at 600 K to generate 100 initial random structures. SA calculations were carried during 20 ps (20000 steps, 1 fs long) as described elsewhere. First, the temperature was risen quickly and was maintained at 600 K for the first 5000 steps, then

the system was cooled gradually from 600 K to 100 K from step 5001 to 18000 and finally the temperature was brought to 0 K during the 2000 remaining steps. For the 3000 first steps, the force constant of the distance restraints was increased gradually from 2.0 kcal.mol^{-1}Å to 20 kcal.mol^{-1}Å. For the rest of the simulation (step 3001 to 20000), the force constant is kept at 20 kcal.mol^{-1}Å. The calculations were launched using the generalized born solvation model. The 20 lowest energy structures with no violations > 0.3 Å were considered as representative of the peptide structure. The representation and quantitative analysis were carried out using Ptraj, MOLMOL[7] and PyMOL (Delano Scientific).

Tables S1: 1H NMR chemical shifts for compound 2 in PBS/D2O (95/5), pH 6.8 at 298 K.

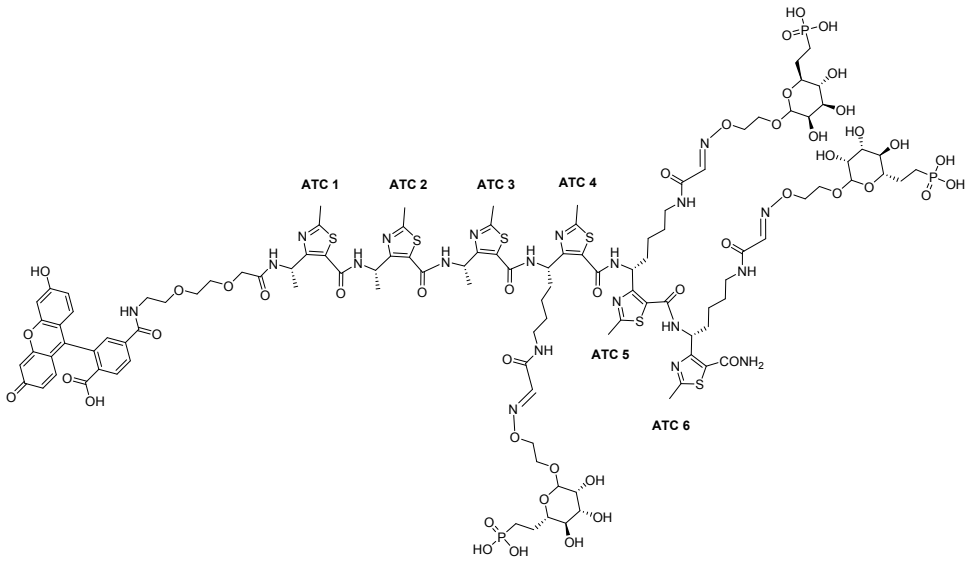

ATC number	HN	$^{\gamma}$CH	$^{\delta}$CH	Others
ATC. 1	8.20	5.26	1.33	$^{\tau 1}CH_3$ nd
ATC. 2	9.15	5.35	1.38	$^{\tau 1}CH_3$ 2.64
ATC. 3	9.17	5.51	1.5	$^{\tau 1}CH_3$ 2.63
ATC. 4	9.32	5.33	2.08	$^{\varepsilon}CH_2$ 1.56 $^{\zeta}CH_2$ 1.71 $^{\eta}CH_2$ 3.76-3.94 NH 8.18 $^{\tau 1}$2.57
ATC. 5	10.09	5.31	2.06	$^{\varepsilon}CH_2$ 1.56 $^{\zeta}CH_2$ 1.70 $^{\eta}CH_2$ 3.54-3.75 NH 8.65 $^{\tau 1}$2.56
ATC. 6	10.14	5.43	2.06	$^{\varepsilon}CH_2$ 1.29-1.36 $^{\zeta}CH_2$ 1.57 $^{\eta}CH_2$ 3.26 NH 8.48 $^{\tau 1}$2.58
NH_2	7.59 - 8.56	-	-	-
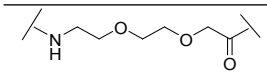 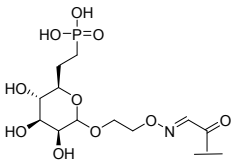	8.56	-	-	CH_2NH 5.64 CH_2 3.74 CH_2 3.80 CH_2 4.00 CH_2CO 3.80 CH_2O 3.75 CH_2ON 4.3 NCH 7.5

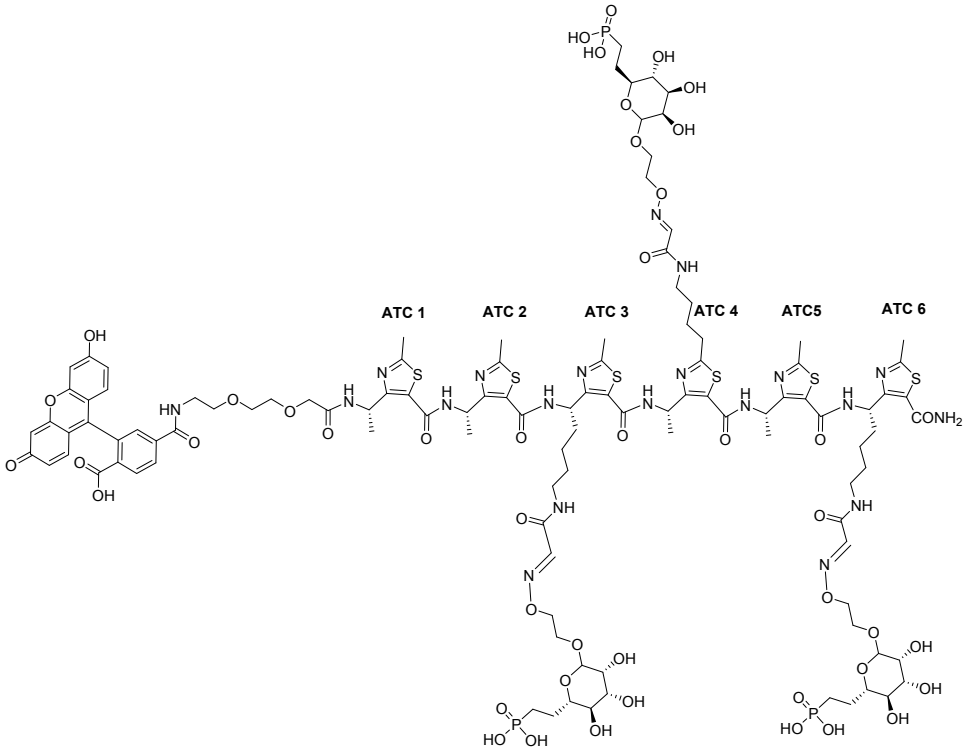

Tables S2: 1H NMR chemical shifts for compound 3 in PBS/D2O (95/5), pH 6.8 at 298 K.

ATC number	HN	$^{\gamma}$CH	$^{\delta}$CH	Others
ATC. 1	8.23	5.32	1.33	$^{\tau 1}CH_3$ nd
ATC. 2	9.19	5.40	1.40	$^{\tau 1}CH_3$ 2.63
ATC. 3	9.40	5.18	1.80-1.90	$^{\varepsilon}CH_2$ 1.10-1.02 1 $^{\zeta}CH_2$ 1.28-0.90 $^{\eta}CH_2$ 3.01 $^{\tau 1}CH$ 2.62$^{\tau 1}$ NH 8.13
ATC. 4	9.59	5.62	1.49	$^{\tau 1}CH_2$ 2.94 $^{\tau 2}CH_2$ 1.51 $^{\tau 3}CH_2$ 1.67 $^{\tau 4}CH_2$ 3.16 $^{\tau 5}$NH 8.33
ATC. 5	9.37	5.74	1.55	$^{\tau 1}CH_3$ 2.63
ATC. 6	9.61	5.41	1.26 - 1.30	$^{\varepsilon}CH_2$ 1.53 $^{\zeta}CH_2$ 1.97 $^{\eta}CH_2$ 3.21 $^{\tau 1}$CH 2.61 NH 8.36
NH_2	7.52 - 8.44	-	-	-
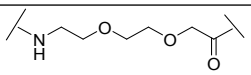 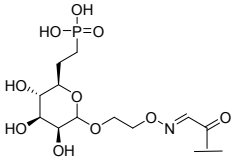	8.64	-	-	CH_2NH 3.63 CH_2 3.8 CH_2 3.53-3.92 CH_2 4.00 CH_2CO 4.01-3.7 CH_2O 3.75 CH_2ON 4.3 NCH 7.5

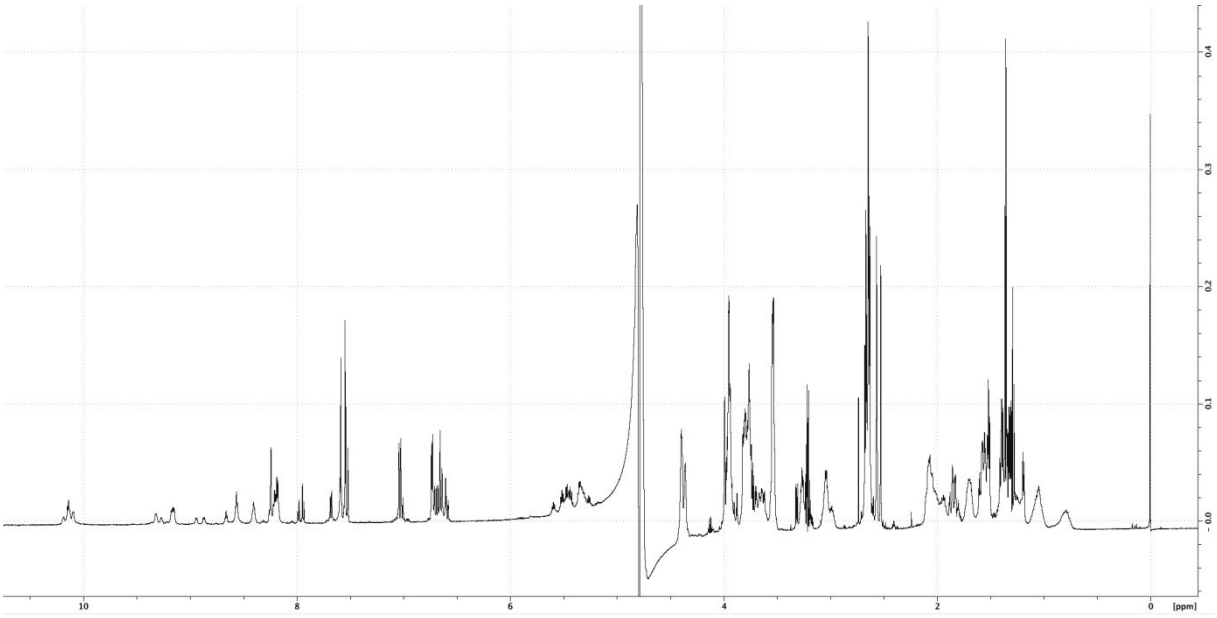

Figure S1: 1H NMR spectrum of compound **2** in PBS/D2O (95/5), pH 6.8 at 298 K.

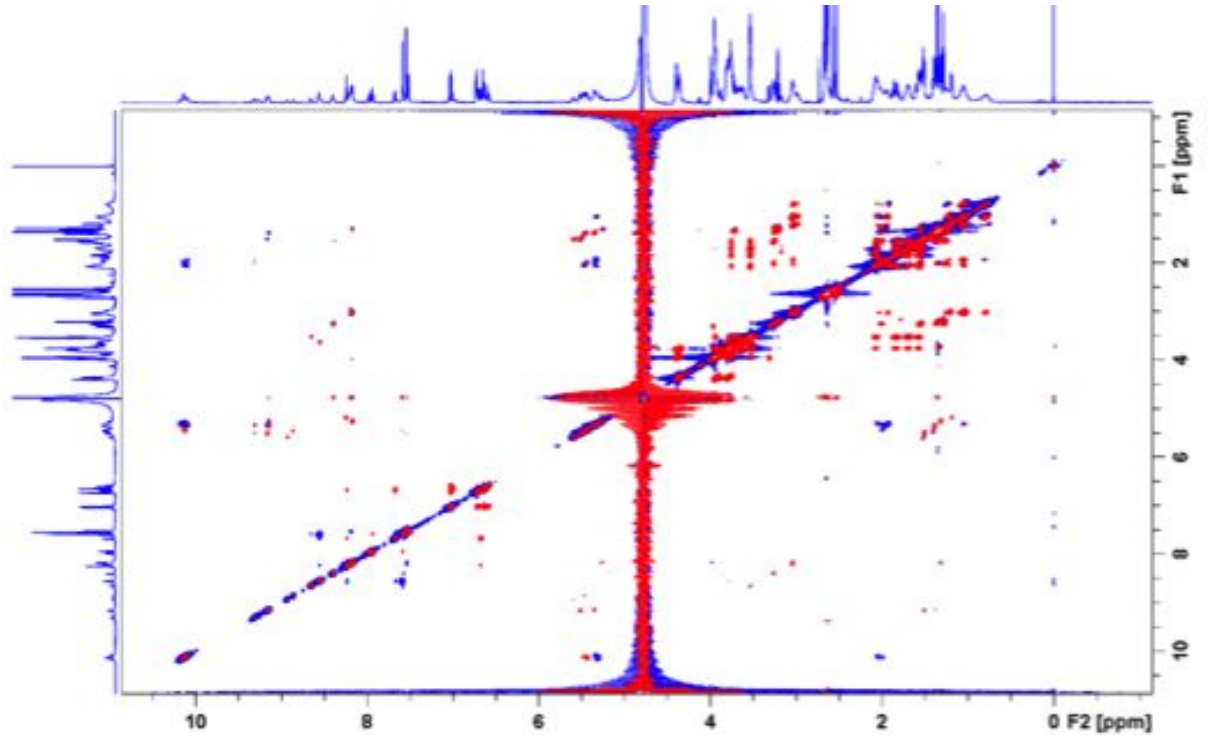

Figure S2: Superimposition of NOESY (blue) and TOCSY (red) spectra of compound 2 in PBS/D2O (95/5), pH 6.8 at 298 K.

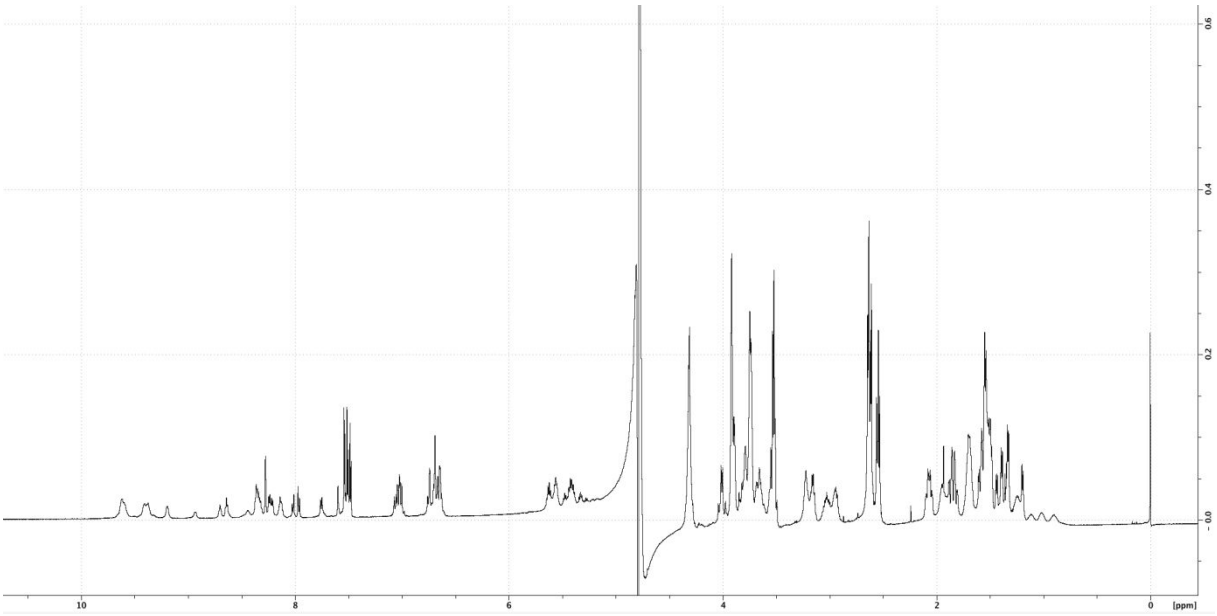

Figure S3: 1H NMR spectrum of compound **3** in PBS/D2O (95/5), pH 6.8 at 298 K.

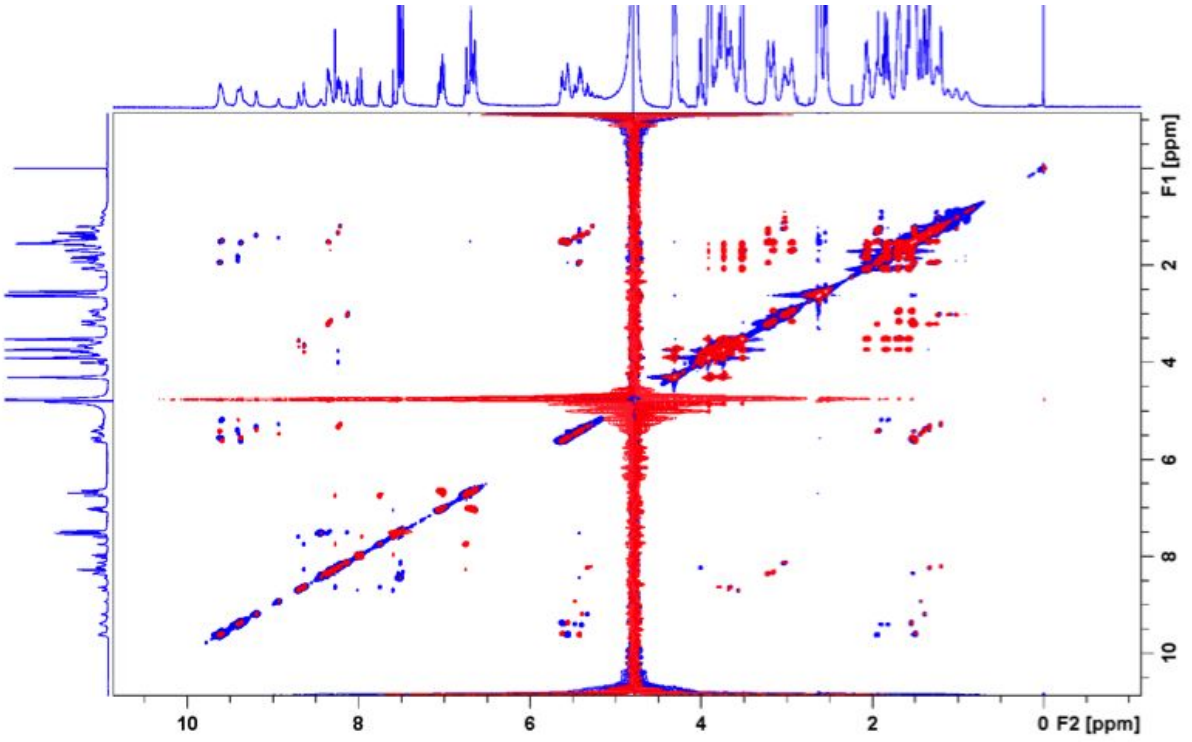

Figure S4: Superimposition of NOESY (Blue) and TOCSY (red) spectra of compound **3** in PBS/D2O (95/5), pH 6.8 at 298 K.

Table S3: Inter-residue NOE correlations in **2** observed in the ROESY spectrum in PBS/D2O (95/5), pH 6.8 at 298 K. Strong < 2.7 Å. 2.7 Å < Medium < 3.3 Å. 3.3 Å < Weak.

NOE correlations	**Intensity**	**Type**
1.NH-2.NH	nd	sequential
2.NH-3.NH	nd	sequential
3.NH-4.NH	nd	sequential
4.NH-5.NH	nd	sequential
5.NH-6.NH	nd	sequential
6.NH-NH_2	nd	sequential
1.Hγ-2.NH	s	sequential
2.Hγ-3.NH	s	sequential
3.Hγ-4.NH	s	sequential
4.Hγ-5.NH	s	sequential
5.Hγ-6.NH	s	sequential
6.Hγ- NH_2	s	sequential
1.Hγ-2.$^{\tau 1}CH_3$	w	sequential
2.Hγ-3.$^{\tau 1}CH_3$	w	sequential
3.Hγ-4.$^{\tau 1}CH_2$	w	sequential
4.Hγ-5.$^{\tau 1}CH_2$	w	sequential
5.Hγ-6.$^{\tau 1}CH_2$	w	sequential
1.Hδ-2.$^{\tau 1}CH_3$	w	sequential
2.Hδ-3.$^{\tau 1}CH_3$	w	sequential
3.Hδ-4.$^{\tau 1}CH_2$	w	sequential
4.Hδ-5.$^{\tau 1}CH_2$	w	sequential
5.Hδ-6.$^{\tau 1}CH_2$	nd	sequential

nd: not detected

Table S4: Inter-residue NOE correlations in **2** observed in the ROESY spectrum in PBS/D2O (95/5), pH 6.8 at 298 K. Strong < 2.7 Å. 2.7 Å < Medium < 3.3 Å. 3.3 Å < Weak.

NOE correlations	**Intensity**	**Type**
1.NH-2.NH	nd	sequential
2.NH-3.NH	nd	sequential
3.NH-4.NH	nd	sequential
4.NH-5.NH	nd	sequential
5.NH-6.NH	nd	sequential
6.NH-NH_2	nd	sequential
1.Hγ-2.NH	s	sequential

2.Hγ-3.NH	s	sequential
3.Hγ-4.NH	s	sequential
4.Hγ-5.NH	s	sequential
5.Hγ-6.NH	s	sequential
6.Hγ- NH_2	m	sequential
1.Hγ-2. $^{\tau 1}CH_3$	w	sequential
2.Hγ-3. $^{\tau 1}CH_3$	w	sequential
3.Hγ-4. $^{\tau 1}CH_2$	w	sequential
4.Hγ-5. $^{\tau 1}CH_2$	w	sequential
5.Hγ-6. $^{\tau 1}CH_2$	w	sequential
1.Hδ-2. $^{\tau 1}CH_3$	w	sequential
2.Hδ-3. $^{\tau 1}CH_3$	w	sequential
3.Hδ-4. $^{\tau 1}CH_2$	w	sequential
4.Hδ-5. $^{\tau 1}CH_2$	w	sequential
5.Hδ-6. $^{\tau 1}CH_2$	w	sequential

nd: not detected

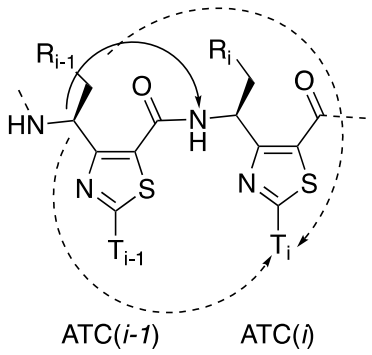

Figure S5: Sequential NOEs correlations observed in NOESY spectra of **2** and **3** consistent with the formation of a C_9-Helix in ATCs Oligomers. Strong NOEs intensity (Plain), weak NOEs intensity (Dashed).

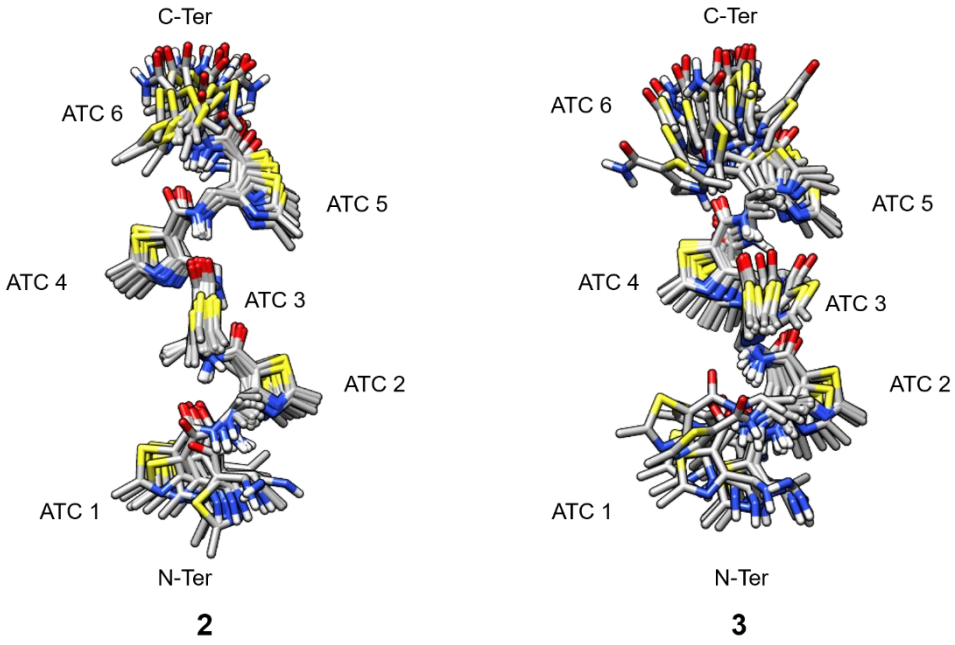

Figure S6: Superimposition on the backbone heavy atoms of the 15 lowest energy NMR solution structures of **2** (RMSD: 0.68) and **3** (RMSD: 1.3) in PBS. For clarity linker and fluorescein have been omitted.

Table S5: Backbone dihedral angles (°) of **2** NMR structures in PBS. Values are ordered from *N*- to *C*-Ter and are average on the 15 lowest energy NMR structures.

Residue	**ϕ**	**θ**	ζ	**ψ**
1	-74.8 ± 28	+119.9 ± 17	-7.8 ± 3.3	-21.2 ± 9.3
2	-77.4 ± 24.3	+128.3 ± 13.3	-7.7 ± 4.7	-22.7 ± 12.5
3	-73.4 ± 17.8	+121.5 ± 5.4	-8.9 ± 2.3	-24.9 ± 3.7
4	-65.8 ± 6.2	+128.7 ± 3.8	-10.7 ± 2.0	-31.2 ± 3.6
5	-73.5 ± 15.5	+123.2 ± 7.3	-8.3 ± 1.9	-26.9 ± 3.8
6	-83.5 ± 18.8	+120.6 ± 16.4	-7.1 ± 2.8	+17.3 ± 7.6

Table S6: Backbone dihedral angles (°) of **3** NMR structures in PBS. Values are ordered from *N*- to *C*-Ter and are average on the 15 lowest energy NMR structures.

Residue	**ϕ**	**θ**	ζ	**ψ**
1	-74.8 ± 28	+120.6 ± 20	-7.9 ± 3.9	-21.4 ± 9.7
2	-85.6 ± 31.1	+132.6 ± 18.9	-6.9 ± 4.0	-20.3 ± 11
3	-78.7 ± 23.68	+122.4 ± 8.8	-8.4 ± 2.7	-25.4 ± 5.2
4	-78.7 ± 25	+116.9 ± 12.0	-7.4 ± 3.4	-22.9 ± 5.0
5	-67.4 ± 15.9	+128.0 ± 10.0	-8.6 ± 1.2	-25.7 ± 2.4
6	-70.9 ± 8.2	+128.4 ± 10.2	-1.6 ± 7.1	-4.8 ± 18

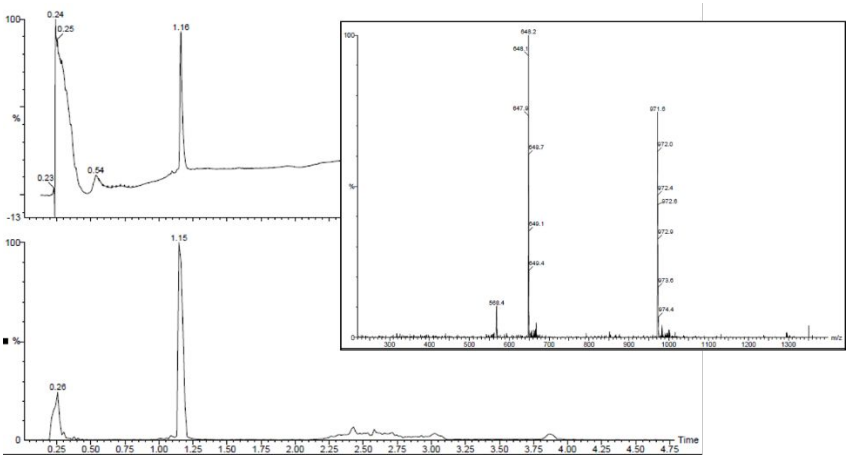

Figure S7: LC-MS traces of **1**

T_R (LC-MS) = 1.16 min; **MS (ESI)**: *m/z* = 648.2 [(M+3H) $^{3+}$], 971.6 [(M+2H) $^{2+}$]

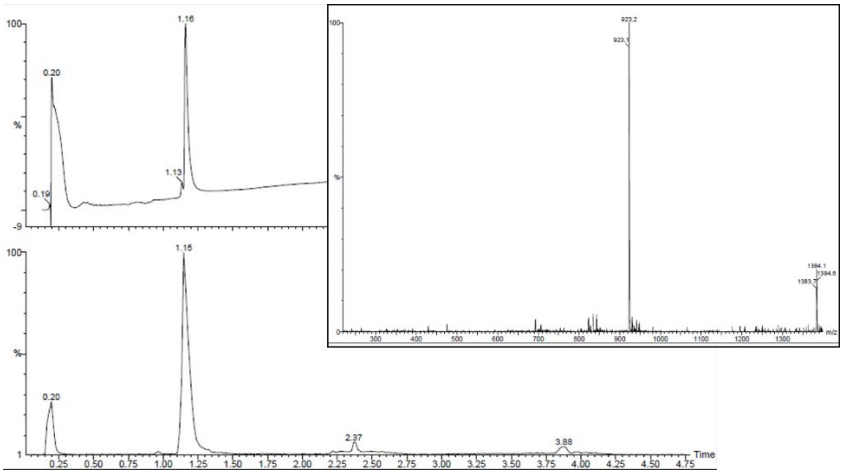

Figure S8: LC-MS traces of **2**

T_R (LC-MS) = 1.16 min; **MS (ESI)**: *m/z* = 923.2 [(M+3H) $^{3+}$], 1384.1 [(M+2H) $^{2+}$]

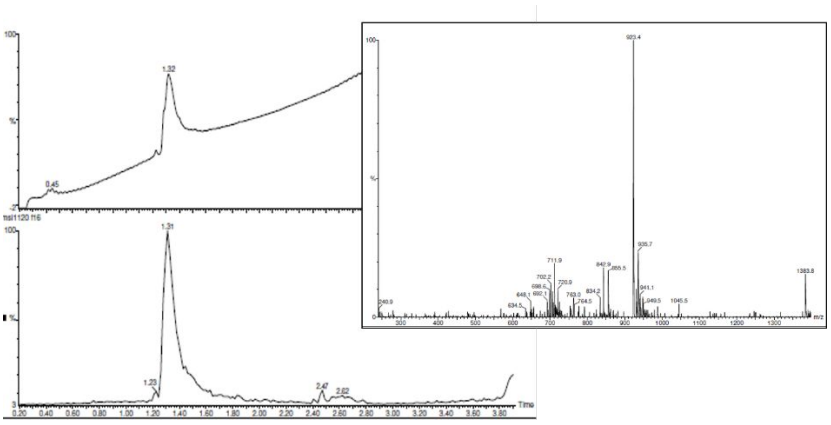

Figure S9: LC-MS traces of **3**

T_R (LC-MS) = 1.32 min; **MS (ESI)**: *m/z* = 923.4 [$(M+3H)^{3+}$], 1383.8 [$(M+2H)^{2+}$]

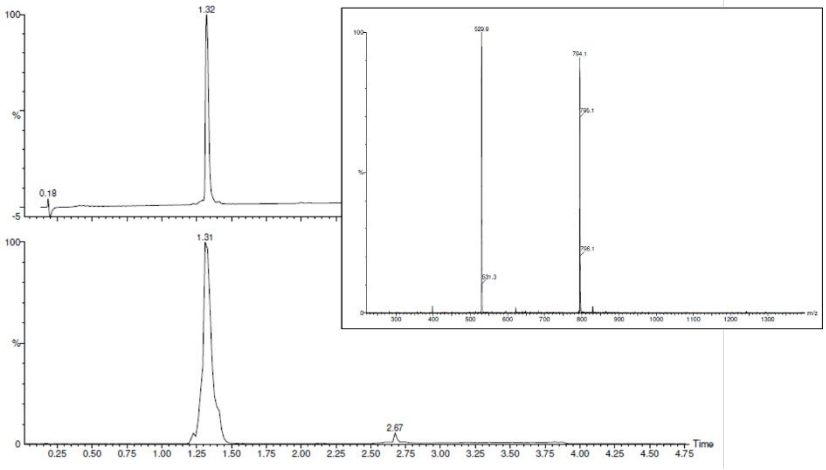

Figure S10: LC-MS traces of **4**

T_R (LC-MS) = 1.32 min; **MS (ESI)**: *m/z* = 529.9 [$(M+3H)^{3+}$], 794.1 [$(M+2H)^{2+}$]

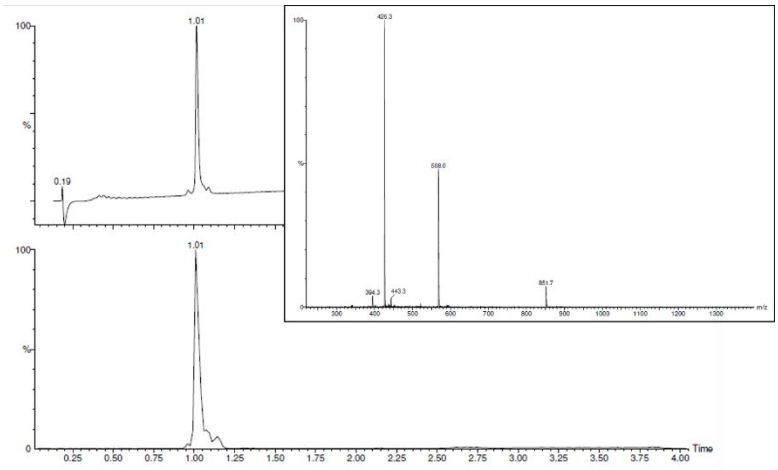

Figure S11: LC-MS traces of **5**

TR (LC-MS) = 1.01 min; **MS (ESI)**: *m/z* = 426.3 [(M+4H) $^{4+}$], 568.0 [(M+3H) $^{3+}$], 851.7 [(M+2H) $^{2+}$]

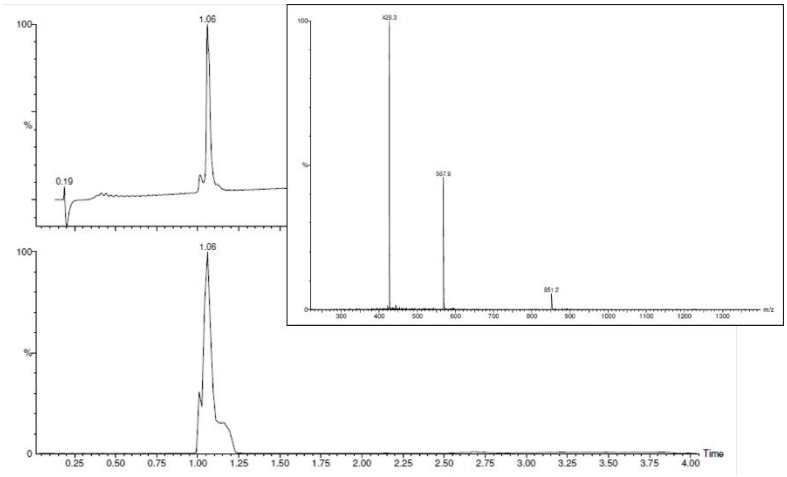

Figure S12: LC-MS traces of **6**

TR (LC-MS) = 1.06 min; **MS (ESI)**: *m/z* = 426.3 [(M+4H) $^{4+}$], 567.9 [(M+3H) $^{3+}$], 851.2 [(M+2H) $^{2+}$]

III. Cellular uptake experiments

Cell culture

Human prostate carcinoma LNCaP cell line cultured in RPMI culture medium supplemented with 10% fetal bovine serum, 1% HEPES, 1% sodium pyruvate and 1% antibiotic (penicillin/streptomycin).

Human umbilical vein endothelial cells (HUVECs) were maintained in Endothelial cell Growth Medium 2 supplemented with fetal calf serum (2%), epidermal growth factor (5 ng mL^{-1}), basic fibroblast growth factor (10 ng mL^{-1}), insulin-like growth factor (20 ng mL^{-1}), vascular endothelial growth factor (0.5 ng mL^{-1}), ascorbic acid (1 µg mL^{-1}), heparin (22.5 µg mL^{-1}), hydrocortisone (0.2 µg mL^{-1}), penicillin (100 U mL^{-1}) and streptomycin (100 µg mL^{-1}).

These cells were grown in humidified atmosphere at 37°C and under 5% CO_2.

Qualitative cellular uptake

The cellular uptake experiment was performed using confocal fluorescence microscopy on living cells. LNCaP cells or HUVECs were plated on Lab-Tek II Chambered Coverglass (Nalge Nunc International Ref 155382) in 0.5 mL culture medium for 24 h. Then, cells were treated with different concentrations of glycosylated conjugates or non-glycosylated counterparts for 24 h. Control cells were treated with vehicle. Fifteen minutes before the end of incubation, cells were stained with CellMaskTM Orange plasma membrane stain (Invitrogen, Cergy Pontoise, France, C10045) for membrane staining at a final concentration of 5 µg mL^{-1}. At the same time, nuclei were stained with Hoechst 33342 at a final concentration of 5 µg mL^{-1}. Then cells were washed two times with culture medium. Confocal fluorescence microscopy was performed on living cells under a 488 nm wavelength excitation for FITC labeled conjugates, 750 nm for nuclei and 561 nm for cell membranes.

Quantitative cellular uptake using FACS.

LNCaP cells were seeded in 12- well plates and let to grow for 24 h. After 24 h of cell growth, cells were treated with different concentrations (10 µM, 1 µM, 0.5 µM, 0.1 µM and 0.01 µM) of **2, 3, 5** and **6** and incubated for 24 h. After 24 h of treatment, cells were harvested and suspended in DPBS containing $MgCl_2$ and $CaCl_2$, Propidium iodide (PI) was added just before sample analysis in the flow cytometer at a final concentration 1 mg mL^{-1}. Flow cytometric analysis was performed using NovoCyte flow cytometer and the data were

analyzed by NovoExpress software (ACEA Biosciences, Inc.). The evaluation of the internalization was carried out in 20,000 events.

Quantitative cellular uptake Kinetics using FACS.

LNCaP cells were seeded in 12-well plates and let to grow for 24 h. After 24 h of cell growth, cells were treated with 10 μM concentration of **2, 3, 5** and **6** and incubated for different time intervals (48 h, 24 h, 18 h, 6 h and 3 h). After the end of incubation time, cells were harvested and suspended in DPBS containing $MgCl_2$ and $CaCl_2$, Propidium iodide (PI) was added just before sample analysis in the flow cytometer at a final concentration 1 mg mL^{-1}. Flow cytometric analysis was performed using NovoCyte flow cytometer and the data were analyzed by NovoExpress software (ACEA Biosciences, Inc.). The evaluation of the internalization was carried out in 20,000 events.

Co-localization study.

The co-localization experiment was performed using confocal fluorescence microscopy on living cells. LNCaP cells were plated onto Lab-Tek II Chambered Coverglass (Nalge Nunc International Ref 155382) in 0.5 mL culture medium for 24 h. Then, human cancer cells were treated with 40 μM concentration of glycosylated conjugates or non-glycosylated counterparts labeled with FITC for 24 h. Control cells were treated with vehicle. Two hours before the end of incubation, cells were treated with 75 nM concentration of LysoTracker® Red DND-99 (Invitrogen) at 37 ºC. Fifteen minutes before the end of incubation, nuclei were stained with Hoechst 33342 at a final concentration of 5 μg mL-1. Then cells were washed two times with culture medium. Confocal fluorescence microscopy was performed on living cells under a 488 nm wavelength excitation for FITC labeled conjugates, 750 nm for nuclei and 577 nm for endolysosomal compartments.

Inhibition of endocytosis with mannose 6-phosphate (M6P).

To study the specificity of **2** to internalize into prostate cancer cells (LNCaP) through CI-MPR, two different experiments were carried out. First, a qualitative method using confocal microscope was performed. For this LNCaP cells were plated onto Lab-Tek II Chambered Coverglass (Nalge Nunc International Ref 155382) in 0.5 mL culture medium for 24 h. Then, human cancer cells were pre-incubated with or without 10 mM concentration mannose 6-phosphate for 15 min, followed by incubation with 1 μM concentration of Cpd (2) in medium containing 10 mM M6P or does not contain M6P for 24 h. Fifteen minutes before the end of

incubation, cells were stained with CellMaskTM Orange plasma membrane stain (Invitrogen, Cergy Pontoise, France, C10045) for membrane staining at a final concentration of 5 μg mL^{-1}. At the same time, nuclei were stained with Hoechst 33342 at a final concentration of 5 μg mL^{-1}. Then cells were washed twice with culture medium. Confocal fluorescence microscopy was performed on living cells under a 488 nm wavelength excitation for FITC labeled conjugates, 750 nm for nuclei and 561 nm for cell membranes. Secondly, a quantitative method using FACS was performed. LNCaP cells were seeded in 12-well plates and let to grow for 24 h. After 24 h of cell growth, cells were treated with 1 μM concentration of **2** as a positive control for 24 h. for revision experiment, cells were pre-incubated with 10 mM concentration of M6P 15 min, and then incubated with 1 μM of **2** in M6P containing medium for 24 h. After the end of incubation time, cells were harvested and suspended in DPBS containing $MgCl_2$ and $CaCl_2$, Propidium iodide (PI) was added just before sample analysis in the flow cytometer at a final concentration 1 mg mL^{-1}. Flow cytometric analysis was performed using NovoCyte flow cytometer and the data were analyzed by NovoExpress software (ACEA Biosciences, Inc.). The evaluation of the internalization was carried out in 10,000 events.

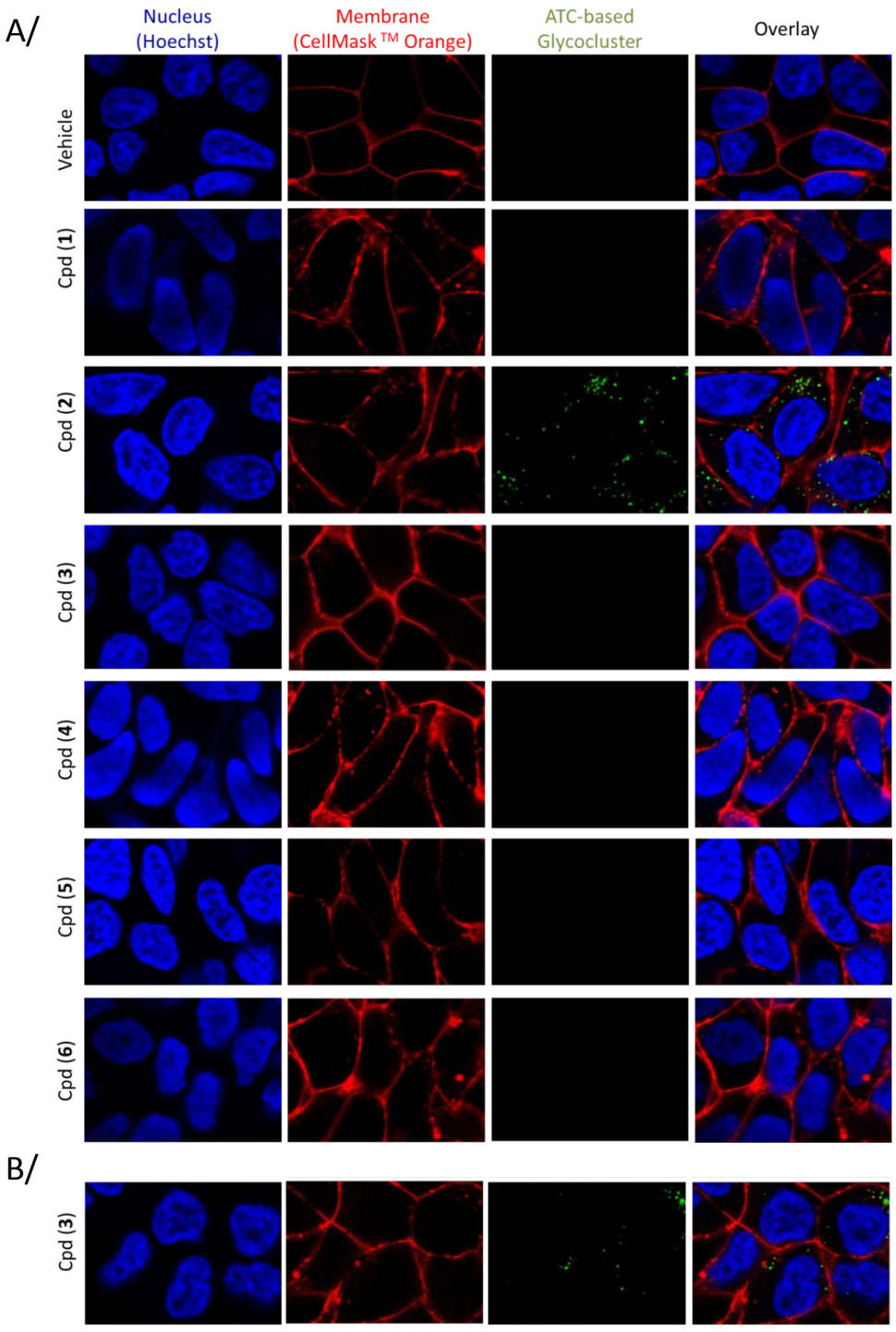

Figure S13: Cellular uptake. Confocal microscopy imaging of living LNCaP prostate cancer cells after 24 h contact with 1 µM oligomers **1-6**. A/ Image acquisition settings: laser power = 1% (maximum laser power: 25 mW). B/ Image acquisition settings: laser power = 7%.

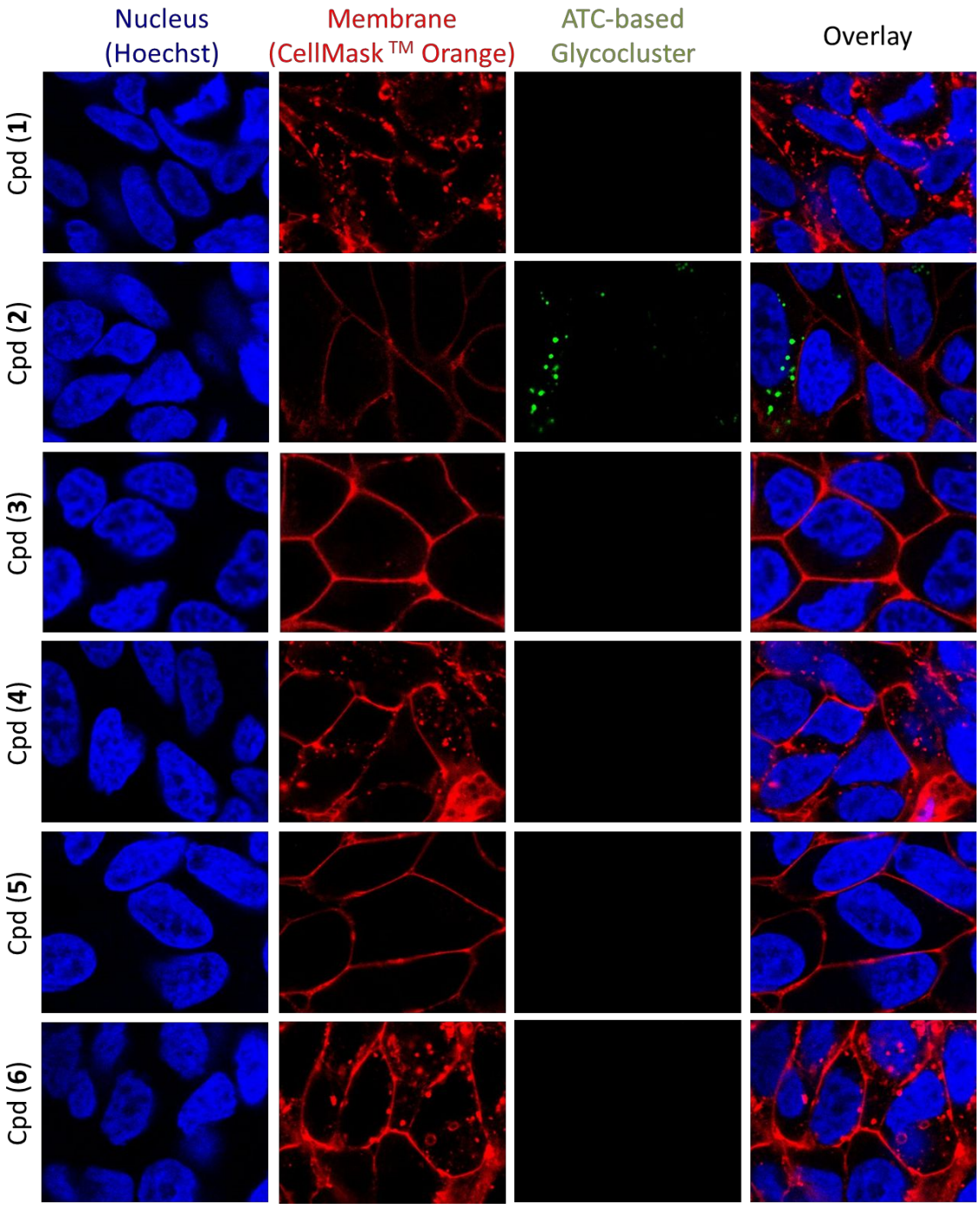

Figure S14: Cellular uptake. Confocal microscopy imaging of living LNCaP prostate cancer cells after 24 h contact with 100 nM oligomers **1-6**. Image acquisition settings: 4% of the maximum power (25 mW).

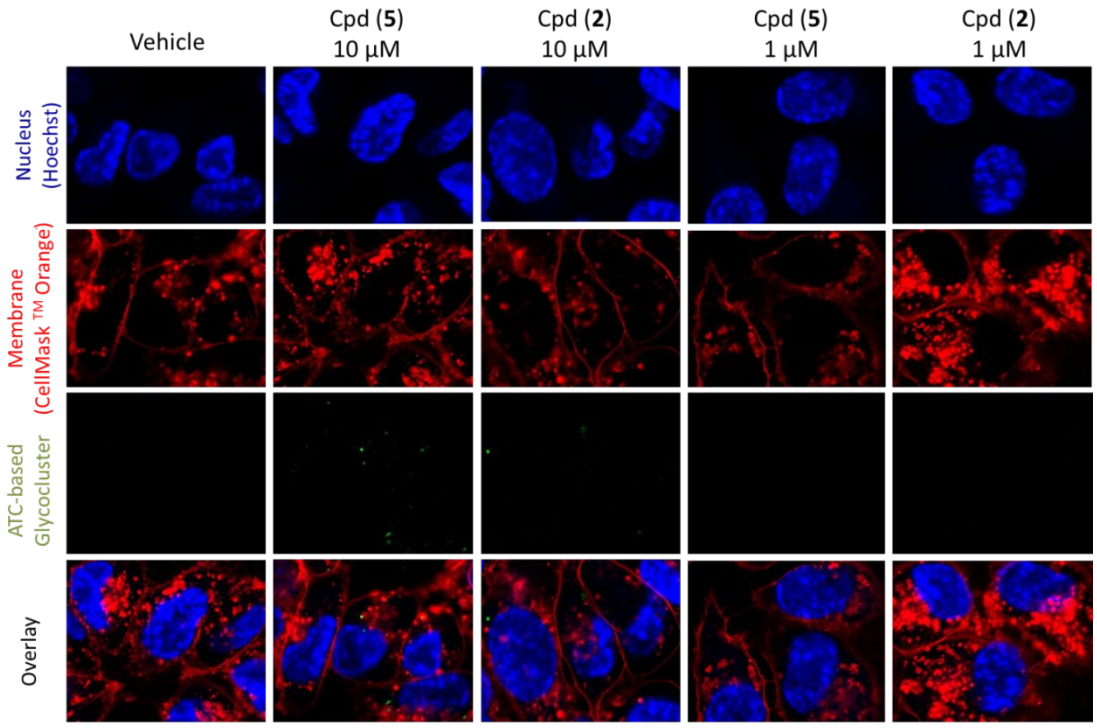

Figure S15. Confocal microscopy imaging of living HUVECs cells after 24 h contact with **2** and **5** at 10 µM and 1 µM. Image acquisition settings: 1% of the maximum power (25 mW).

Affinity for cation-independent mannose 6-phosphate receptor (CI-MPR)

A microtiter plate was absorbed with pentamannose 6-phosphate (PMP) overnight according to a protocol previously described.[8] The compounds were pre-incubated during 2 h with a biotinylated CI-MPR (CI-MPRb) before incubation of the mixture in the microtiter plate previously coated with PMP for 2 h. CI-MPRb linked to PMP was then quantified by streptavidin peroxidase detection. The affinity for CI-MPR was performed at a concentration range from10^{-7} to 10^{-4} M of compounds.

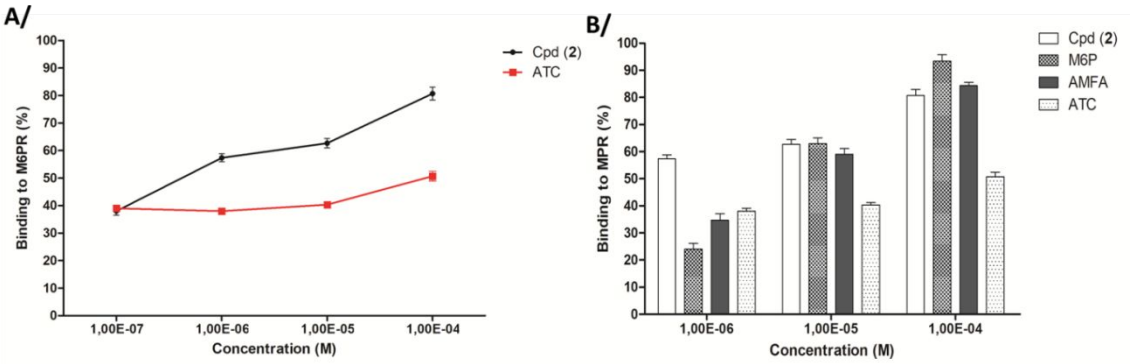

Figure S16. (A) Affinity of **2** and ATC backbone for CI-MPR at different concentrations. (B) IC_{50} determination for **2**, ATC backbone, M6P and AMFA. Results are presented as mean ± SEM (n = 2).

References

(1) Aguesseau, M. Gary-Bobo, M. Garcia, A. Morère and L. T. Maillard (2018) Can Heterocyclic γ-Peptides Provide Polyfunctional Platforms for Synthetic Glycocluster Construction? *Chem. Eur. J.*, 24, 11426-11432.

(2) L. Mathieu, C. Bonnel, N. Masurier, L. T. Maillard, J. Martinez and V. Lisowski (2015) Cross-Claisen Condensation of *N*-Fmoc-Amino Acids – A Short Route to Heterocyclic γ-Amino Acids. *Eur. J. Org. Chem.*, 2262-2270.

(3) Gaussian 09, M. J. Frisch, G. W. Trucks, H. B. Schlegel, G. E. Scuseria, M. A. Robb, J. R. Cheeseman, G. Scalmani, V. Barone, B. Mennucci, G. A. Petersson et al. Gaussian, Inc., Wallingford CT, 2009. *Journal*, 2009.

(4) B. A. Johnson and R. A. Blevins (1994) NMR View: A computer program for the visualization and analysis of NMR data. *J. Biomol. NMR, 4, 603*.

(5) K. Wüthrich (1986) *NMR of Proteins and Nucleic Acids*, John Wiley & Sons, Inc., New-York.

(6) D.A. Case, R.M. Betz, D.S. Cerutti, T.E. Cheatham, III, T.A. Darden, R.E. Duke, T.J. Giese, H. Gohlke, A.W. Goetz, N. Homeyer et al. (2016), AMBER 2016, University of California, San Francisco.

(7) R. Koradi, M. Billeter and K. Wuthrich (1996) MOLMOL: A program for display and analysis of macromolecular structures. *J. Mol. Graph.* **14**, 51-55.

(8) A. Jeanjean, M. Garcia, A. Leydet, J. L. Montero and A. Morere (2006) Synthesis and receptor binding affinity of carboxylate analogues of the mannose 6-phosphate recognition marker. *Bioorg. Med. Chem.*, **14**, 3575-3582